

On the Role of pre-treatment of Aluminum Substrate on Deposition of Cerium Based Conversion Layers and Their Corrosion-Protective Ability

Reni Andreeva¹, Emilia Stoyanova¹, Aleksandar Tsanev², Maria Datcheva³, Dimitar Stoychev^{1,*}

¹ Institute of Physical Chemistry “Rostislav Kaischew”, Bulgarian Academy of Sciences, Acad. G. Bonchev str., Bl. 11, 1113 Sofia, Bulgaria

² Institute of General and Inorganic chemistry, Bulgarian Academy of Sciences, Acad. G. Bonchev str., Bl. 11, 1113 Sofia, Bulgaria

³ Institute of Mechanics, Bulgarian Academy of Sciences, Acad. G. Bonchev str., Bl. 4, 1113 Sofia, Bulgaria

*E-mail: stoychev@ipc.bas.bg

Received: 7 February 2018 / Accepted: 11 April 2018 / Published: 10 May 2018

We've investigated the effect of preliminary Al substrate treatment on the deposition and corrosion-protection ability of thin, conversion cerium oxide layers formed in solutions containing Ce^{3+} and Cu^{2+} ions. The cerium oxide layers and their corrosion protection behaviour were investigated by SEM, EDS, XPS, and model polarization E-Ig i and I-t chronoamperometric curves. We report on the structure, morphology, chemical composition and the state of the elements in the conversion layers, as well as the thickness and distribution of the elements up to the „conversion layer”/”aluminium substrate” interphase boundary. The preliminary treatment of the Al substrate, as well as the presence of Cu^{2+} , both substantially influence the thickness, composition and protective ability of the formed ceria and alumina mixed conversion layers. All these features are related to changes in the ratio of the formed AlOOH ($\sim\text{Al}_2\text{O}_3\cdot\text{H}_2\text{O}$), $\text{Ce}(\text{OH})_3$ ($\sim\text{Ce}_2\text{O}_3$) and $\text{Ce}(\text{OH})_4$ ($\sim\text{CeO}_2$) on the modified Al surface, which are affected by the preliminary treatment of the Al substrate and presence of Cu^{2+} ions in the immersion treatment solution based on Ce^{3+} ions.

Keywords: Aluminium, Pre-treatment, Conversion layers, Cerium oxides, Corrosion protection

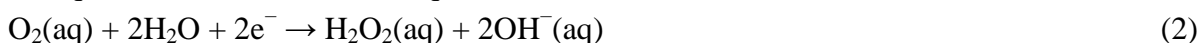
1. INTRODUCTION

The chemically deposited conversion layers on aluminium and its alloys are among the most widely used (separately or in combination with painting lacquer coatings having excellent adhesion) for corrosion protection of articles, made of these materials [1]. For ever 50 years the leading technologies for their conversion anticorrosion treatment have been based on solution compositions,

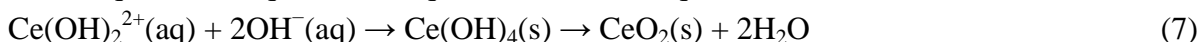
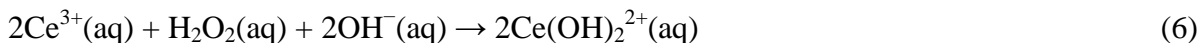
containing six-valent chromium. Despite the fact that they have already proved their exceptional effectiveness, their exploitation was terminated, due to their high toxicity and carcinogenicity, in accordance with the changing legislation in health and environmental protection [2]. Therefore, intensive investigations are being carried out to replace the electrolytes, containing Cr^{6+} ions with Cr^{3+} ions [3,4] or with some other less toxic and inexpensive metal salts, which are abundantly occurring in nature [5-10]. Special interest is paid to those electrolytes and respective methods, that include salts of lanthanide metals, since the protective oxide/or hydroxide coatings, formed on their basis are among the least toxic and the ingestion or inhalation is not considered harmful for health [11-13]. The pioneering studies of Hinton and co-authors resulted in the elaboration of the so called “cerate coating” processes [14,15] for protection from corrosion of different aluminum alloys. They involved Ce^{3+} ions, as well as the strong oxidizing agent H_2O_2 in the working solution, leading to an increase in the rate of the process of oxidation of Ce^{3+} to Ce^{4+} in the solution. This fact, in turn, determines increase the content of fourth-valency cerium in the conversion layer [16]. A series of some systematic investigations have been carried out and they are reported in references [17-28].

Because in the present study our interest was focused on the simple, more stable, free of oxidizing agent(s) and convenient in work solutions, we would like to point briefly out the following.

According to ref. [8], [17], [25], [26] and [29], the formation of conversion protective cerium oxide films on aluminum and on its alloys from solutions of simple salts of cerium at pH close to the neutral value, *to which no oxidizing agent (H_2O_2) has been added*, can be accomplished involving the participation of oxygen, dissolved in them. The summarized mechanism, based on these concepts, which is given in [29 and references there in], supposes the simultaneous occurrence of conjugated reactions of reduction of oxygen on the active cathodic sections and anodic oxidation (dissolution) of the aluminum substrate, described by equations 1-4:



The occurrence of these processes leads to the formation of $\text{Ce}(\text{OH})_2^{2+}$ complexes in the solution. Their solubility, as a consequence of the strong local alkalization of the aluminium surface, is considerably lower, which leads to their precipitation and formation of a final product CeO_2 (more specifically - according to [6,9,12,31] – a mixture of CeO_2 and Ce_2O_3) on the aluminum surface, in accordance with the equations 5 – 7 [29].

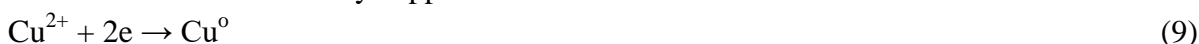


As it was pointed out in the schematic representation shown in [26], “a non-insulating alumina layer allowing Faradaic processes is therefore necessary for CeO_2 deposition to occur”. Obviously, in our case (absence of H_2O_2 as a precursor in the working solution for immersion treatment of Al substrate) the oxidation of Al on the anodic sites (eq.3) and reduction of O_2 on the cathodic sites induces the evolution of H_2O_2 and the increase in pH (eq.1, 2). This can lead to the precipitation of a final product $\text{Ce}(\text{OH})_3$ in accordance with the equation 8 [29]:



Moreover, one should take into account, that depending on the chemical composition of the aluminum substrate and the type of the preliminary treatment, zones varying in their chemical nature and in their electrochemical properties could be appearing on its surface. These zones are characterized by: cathodic sections of intermetallic compounds; pure aluminum surface having anodic behavior and sections of $\text{Al}(\text{OH})_3/\text{Al}_2\text{O}_3$ on incompletely deoxidized aluminum surface which are having cathodic behavior in the case of consecutive conversion treatment. This heterogeneity following the operations of pretreatment changes the activity of the treated aluminum surface, which appears to be a prerequisite for variation of the rates of the occurring conversion processes during the formation of the protective cerium oxide coatings.

This influence is especially strong in the cases when besides Ce^{3+} , ions of other metals (more positive than the aluminum) are added to the working solution for conversion treatment, as a result of which their reduction on the aluminum surface leads to the formation of additional cathodic sections. For example, when Cu^{2+} ions are added to the solution, per equation 9, there occurs immersion deposition of clusters of elementary copper



which plays the roll of cathodic sections, accelerating the anodic oxidation of Al (reaction 3), determined by the functioning of microgalvanic Al/Cu couples. This favors the proceeding of the cathodic reactions of reduction of oxygen (in accordance with equations 1 and 2), leading to the formation of OH^{-} and H_2O_2 species in the volume of the solution for conversion treatment and local alkalization of the aluminum surface. This results in creation of even more favorable conditions for precipitation of cerium oxides and hydroxides on the aluminum surface, in accordance with equations 5-7.

In parallel with the investigations aimed at the optimization of the solution composition and the conditions for currentless deposition of the conversion cerium oxide protective layers on Al and on its alloys, studies are also being carried out actively with respect to clarifying the role and the options for improving the quality and the protective ability of this type of conversion coatings by optimizing the so called "pretreatment" and "post-treatment" processes [17,21,22]. Here, the following should be taken into account:

- the further elucidation and the improvement of the effect of preliminary treatment of the aluminium surface (the processes of degreasing and deoxidation) – prior to the deposition of the conversion cerium oxide layers [28, 32-35];
- inclusion of processes of additional chemical treatment of cerium oxide layers, with the purpose to promote their protective ability, after (or during) its deposition on the aluminium surface.

The data available in the current literature, show that the different pre-treatments of Al substrate greatly improved the corrosion resistance of the “conversion ceria layers/Al substrate” system, including decrease in local damages and pitting formation, but they do not give us sufficiently clarified concepts for their role and their effects. In this aspect, the aim of the present study was to investigate: 1) the changes in the chemical composition and chemical state of the elements on the surface of the technically pure aluminum substrate in the course of their consecutive pretreatment in

alkaline and in acidic solutions; 2) the influence of these pretreatment processes on the occurrence of the conversion processes of deposition of cerium oxide layers and on the corrosion protective ability of the “conversion ceria layers/Al substrate” system.

2. EXPERIMENTAL

Layers of cerium oxide (chemical conversion treatment) were deposited on substrates of “technically pure” Al 1050 (containing 0.40% Fe, 0.25% Si, 0.05% Mn, 0.05% Cu, 0.07% Zn, 0.05% Mg) selected by us as a model object, which finds wide application as a construction material. The studied samples of dimensions 1x1 cm, were cut out of Al sheets of thickness 0.1 cm. They were suspended on wire jigs, made of the same type of Al. Their pre-treatment involved degreasing in organic solvent, degreasing (chemical cleaning) in aqueous solution of NaOH - or chemical cleaning in NaOH and consecutive etching and surface activation in HNO₃ (acidic deoxidation) at room temperature as described in [36]. After each one of these operations, the obligatory standard rinsing of the samples was accomplished with distilled water.

Taking into account the considerations of Decroly and Petitjeanse ([26] and references there in), as well as the results of our previous studies [31, 36-38] with respect to the possible influence of pH, time interval of conversion, nature of counter ion (anion), buffer, concentration of catalysts and surfactants, temperature of conversion solution, time interval of immersion, etc., we chose to investigate the formation of conversion Ce-containing protective oxide layers of two types using possibly the simplest solutions containing: 1) CeCl₃·5x10⁻¹M and 2) CeCl₃·5x10⁻¹M + CuCl₂ – 1.10⁻⁵M. No H₂O₂, or other type of oxidizing agent, was added. The investigations were carried out at pH=4.1, temperature of deposition 25°C and time interval of deposition 120 min. Upon choosing to work with these solutions we took into account the data, reported in [37], in accordance with which at concentration of CuCl₂ 1.10⁻⁵M in the working solution, the clusters and agglomerates deposited by immersion on the aluminum surface [39] are covering it uniformly. The abbreviated titles of the studied samples are given in Table 1.

Table 1. Basic components of the solutions for pretreatment operations and conversion treatment and respective Abbreviated titles of the obtained samples subject to investigation.

Pretreatment operation of the Al substrate in aqueous solutions of:	Conversion treatment in aqueous solutions of:	Abbreviated titles of the obtained sample subject to investigation
1.5M NaOH	0.5M CeCl ₃ ·7H ₂ O	CeO _x CeCl ₃ /Al _{NaOH}
1.5M NaOH and 5M HNO ₃	0.5M CeCl ₃ ·7H ₂ O	CeO _x CeCl ₃ /Al _{NaOH/HNO3}
1.5M NaOH	0.5M CeCl ₃ ·7H ₂ O + 1x10 ⁻⁵ M CuCl ₂ ·2H ₂ O	CeO _x CeCl ₃ +CuCl ₂ /Al _{NaOH}
1.5M NaOH and 5M HNO ₃	0.5M CeCl ₃ ·7H ₂ O + 1x10 ⁻⁵ M CuCl ₂ ·2H ₂ O	CeO _x CeCl ₃ +CuCl ₂ /Al _{NaOH/HNO3}

The morphology, structure and chemical composition of the conversion films, as well as the distribution of the elements on the aluminium surface (prior to and after the deposition of the ceria

protective layers) were observed by electron microscopy (JEOL JSM 6390). It was under the conditions of secondary electron image - SEI, back-scattered electrons -BEC and characteristic energy dispersive X-rays – EDS. The applied voltage was 120 kV, $I \sim 100 \mu\text{A}$) and by X-ray photoelectron spectroscopy (XPS).

The XPS measurements were carried out on AXIS Supra electron-spectrometer (KratosAnalytical Ltd.) using monoichromatic $\text{AlK}\alpha$ radiation, having a photon energy of 1486.6 eV. The analysed area was 0.75 mm^2 . The energy calibration was performed by normalizing the C1s line of adsorbed adventitious hydrocarbons to 285.0 eV. The binding energies (BE) were determined with an accuracy of $\pm 0.1 \text{ eV}$. The changes in composition and chemical surrounding in the depth of the films were determined monitoring the areas and binding energies of C1s, O1s, Al2p, Na1s and N1s photoelectron peaks. The beam power was 500 eV. The sputter rate was calculated according to

$$\dot{z} = \frac{M}{\rho \cdot N_A \cdot e} \cdot S \cdot j_p \left[\frac{m}{s} \right], \text{ where } M - \text{molar mass [kg/mol]}, \rho - \text{density [kg/m}^3\text{]}, N_A - \text{the Avogadro}$$

constant, e - charge of the electron, S – sputtering yield [atom/ion], j_p – primary ion current density [A/m^2]. (According to this equation time of sputtering 1 sec = 0.02 nm thickness of the layer). Using the commercial data-processing software of Kratos Analytical Ltd. the concentrations of the different chemical elements (in atomic %) were calculated by normalizing the areas of the photoelectron peaks to their relative sensitivity factors. The deconvolution was performed using XPS peak free software.

The corrosion behavior of the samples was tested in 0.1M NaCl (“p.a.” Merck) model medium at 25°C. Platinum electrode was used as the counter electrode having dimensions of 10x10x0.6 mm, while the reference electrode was saturated calomel electrode (SCE), ($E_{\text{SCE}} = +0.240\text{V}$ vs. SHE). All the potentials in this study are compared to SCE. The anodic and cathodic polarization curves were obtained by means of a potentiostat/galvanostat Gamry Interface 1000, whereupon the obtained results were processed with the help of specialized software. The curves were recorded at a sweeping rate of the potential $10 \text{ mV}\cdot\text{s}^{-1}$ within the range of potentials from -2500 up to $+2500 \text{ mV}$. Chronoamperometric studies were based on j - t curves obtained for the as-deposited samples after 1 h exposure in 0.1 M NaCl at fixed potential -0.5V versus SCE.

The degree of corrosion protection (z , %) was evaluated on the basis of the following equation (10):

$$z = \frac{(i_{\text{corr(Al)}} - i_{\text{corr(CL/Al)}})}{i_{\text{corr(Al)}}} \times 100, \% \quad (10),$$

where $i_{\text{corr(Al)}}$ is the corrosion current of specimen of Al, non-coated with conversion film, determined from the potentiodynamic polarization curves, while $i_{\text{corr(CL/Al)}}$ is the corrosion current for the system “conversion layer/Al substrate”

3. RESULTS AND DISCUSSION

3.1. SEM and EDS investigations

Figure 1 characterizes the morphology and the structure of the Al substrate, after preliminary degreasing in organic solvent and treatment in: Fig. 1a - alkaline solution of 1,5 M NaOH; Fig.1b - alkaline solution of 1,5 M NaOH and subsequent treatment in deoxidizing 5 M HNO_3 solution. One

can see that it is «decorated» with “observable” iron agglomerates (shown by arrows) of intermetallic phase of the type Al_3Fe [40] whose sizes are bigger after deoxidizing in HNO_3 solution (Fig. 1b). As it is known, from electrochemical point of view, they are identified as cathodic sections.

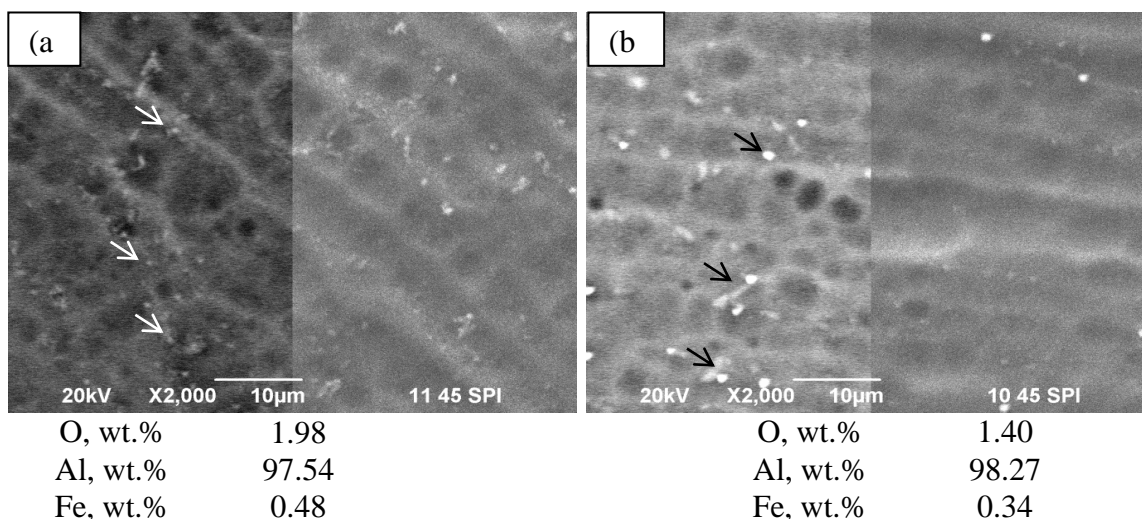


Figure 1. SEM micrograph of the surface of Al substrate (a) after pre-treatment in 1.5M NaOH; (b) after pre-treatment in 1.5M NaOH and in 5M HNO_3 .

Figures 2 and 3 represent the SEM micrographs of the formed conversion cerium-oxide layers (at $t=25^\circ\text{C}$ and time interval of deposition 120 min), illustrating the surface morphology and the structure of the deposited films, depending on the type of preliminary treatment and on the composition of the electrolytes used for chemical conversion treatment. The distribution of the cerium-oxide coating, formed in electrolyte containing CeCl_3 on substrates, which are activated in advance only in NaOH - sample $\text{CeOx}_{\text{CeCl}_3}/\text{Al}_{\text{NaOH}}$ - is less non-homogeneous (Fig. 2a) in comparison with the coating, deposited after consecutive activation in NaOH and deoxidation in HNO_3 - sample $\text{CeOx}_{\text{CeCl}_3}/\text{Al}_{\text{NaOH}/\text{HNO}_3}$ (Fig. 2b). On the basis of the EDS analysis (see data below the figure) of these samples, the concentration of Ce in the deposited conversion layer is 0.63% and 2.79%, respectively, depending on the type of the preliminary treatment. Obviously, these differences in the concentrations are associated with the formed stable AlOOH ($\text{Al}_2\text{O}_3 \cdot \text{H}_2\text{O}$) on the surface of the aluminium substrate in the case of its treatment in aqueous solution of NaOH ($\text{pH} \sim 11.5$).

During the additional treatment in HNO_3 ($\text{pH} \sim 0.5$), the AlOOH ($\text{Al}_2\text{O}_3 \cdot \text{H}_2\text{O}$) formed in the preceding alkaline treatment is being dissolved (in the form of Al^{3+} [30]), as confirmed by the changing concentration of Al and O. As a result, cathodic sections appear on the aluminium surface to a considerably greater extent, representing the denoted intermetallic phase Al_3Fe . This favors the occurrence of reactions 1, 2, 4-6, respectively the formation of the ceria conversion layer.

What is also interesting to note is the fact, that in the case of the samples $\text{CeOx}_{\text{CeCl}_3+\text{CuCl}_2}/\text{Al}_{\text{NaOH}}$ and $\text{CeOx}_{\text{CeCl}_3+\text{CuCl}_2}/\text{Al}_{\text{NaOH}/\text{HNO}_3}$, treated in NaOH and respectively in NaOH and in HNO_3 consecutively, the homogeneity of distribution of the formed conversion layer from electrolyte containing CeCl_3 and CuCl_2 (Fig.3) is higher. Its distribution on the aluminium substrate is more uniform in comparison with the layers formed from electrolyte containing only CeCl_3 (Fig. 2).

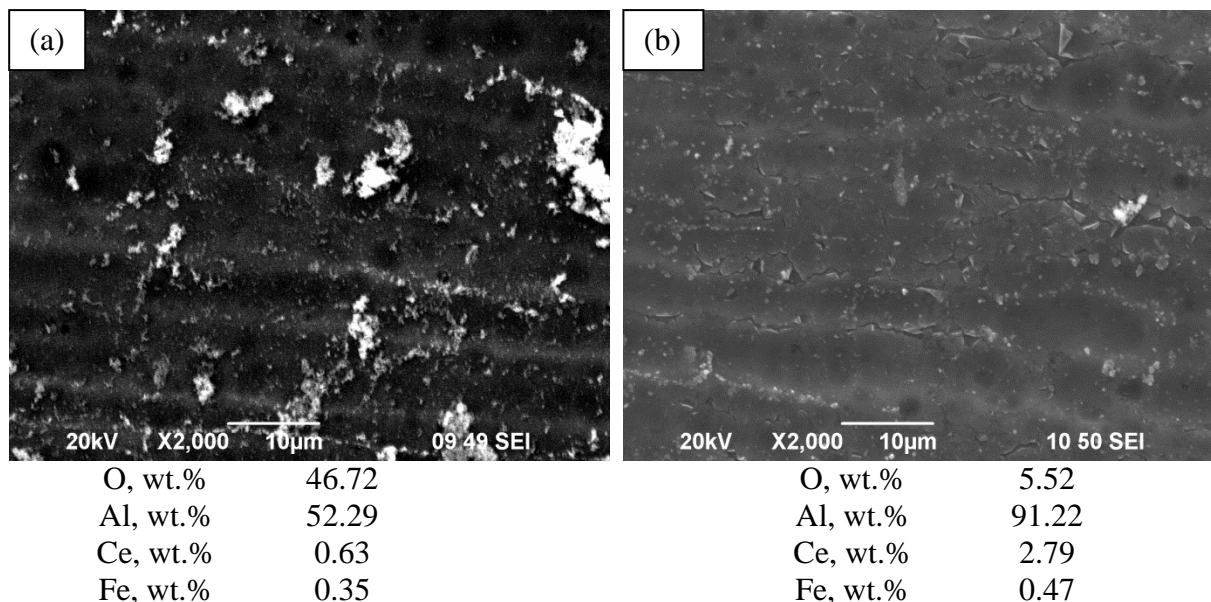


Figure 2. SEM micrographs and EDS data on the surface of the systems $CeO_x/CeCl_3/Al_{NaOH}$ and $CeO_x/CeCl_3/Al_{NaOH/HNO_3}$ obtained after: (a) pre-treatment of Al substrate in 1.5M NaOH; (b) pretreatment of Al substrate in 1.5M NaOH and 5M HNO_3 .

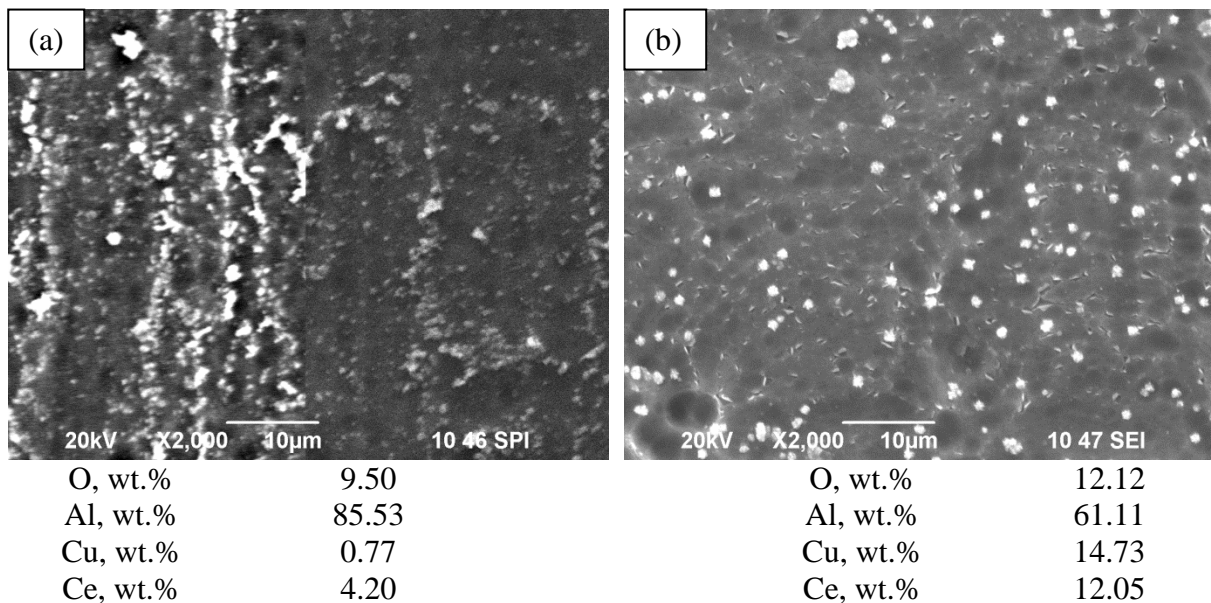


Figure 3. SEM micrograph and EDS data on the surface of the systems $CeO_x/CeCl_3+CuCl_2/Al_{NaOH}$ and $CeO_x/CeCl_3+CuCl_2/Al_{NaOH/HNO_3}$ obtained after: (a) pre-treatment of Al substrate in 1.5M NaOH; (b) pretreatment of Al substrate in 1.5M NaOH and 5M HNO_3

In the presence of Cu^{2+} in the electrolyte and the respective formation of additional copper cathodic sections, the concentrations of cerium and CeO_x on the aluminum surface increase. The EDS analyses in “Point mode” (in areas “ceria/Cu/Al”) have shown up to three or four times higher concentration of ceria on Cu agglomerates [31]. It is significantly higher in comparison with that established in the cases of samples $CeO_x/CeCl_3/Al_{NaOH}$ and $CeO_x/CeCl_3/Al_{NaOH/HNO_3}$, obtained in

electrolyte containing only Ce^{3+} ions. In the case of preliminary treatment of the Al substrate in 1.5M NaOH the EDS analysis established 4.20% Ce (85.53% Al, 9.50% O and 0.77% Cu, respectively) - Fig. 3a, while upon consecutive treatment in solutions of 1.5M NaOH and 5M HNO_3 – the determined concentration of Ce is quite higher - 12.05% (61.11% Al, 12.12% O and 14.73% Cu, respectively) - Fig.3b. This effect, in our opinion, is associated with the immersion deposition of elementary copper on the Al surface (see text showing EDS data under Fig.3), and the respective formation of additional cathodic sections. Obviously, this leads to increase of the active working surface area on the aluminium substrate, enhancing the occurrence of reactions of formation of ceria conversion layers.

3.2. XPS investigations

3.2.1. Investigation of the influence of pre-treatment processes of Al substrate on the chemical composition of its modified surface

We reported in [36] on detailed X-ray photoelectron spectroscopy studies of the influence of pretreatment of “technically pure” Al 1050 in solutions of NaOH and respectively in NaOH and HNO_3 consecutively on transformations of content (chemical composition and state of the elements). The main results showed that:

- only XPS peaks of aluminum, oxygen and sodium (traces from not fully washed NaOH) are present in XPS spectra;
- the depth profiles of studied specimens realized by means of argon etching in the course 15 – 2050 s, and recorded in XPS spectra established (after deconvolution of Al2p and O1s peaks) that the layers are composed of two components - Al_2O_3 and AlOOH. In this case, the surface consists mainly of AlOOH and some smaller amounts of Al_2O_3 , at a ratio of AlOOH/ Al_2O_3 approximately 3.6 : 1, which is preserved in the depth of the surface layer;
- comparing the time intervals for reaching the inter-phase boundary AlOOH+ Al_2O_3 /Al, which are proportional to the thickness of the modified surface layer (as a result of pretreatment of the Al) showed that the thickness of the oxide/hydroxide layer for the substrates treated with NaOH is ~ 2,3 times much bigger [36] in comparison with that of the layer, formed after additional treatment in HNO_3 (see the insert in Fig.4). It is important to point that this thickness is ~ 10 times smaller than the thickness of the surface layers formed after analogous pretreatment on the wide-studied Mg containing Al alloy 7075-T6 substrate [34].

3.2.2. Investigation of the influence of chemical composition of the working solutions on the chemical composition and thickness of deposited conversion layers. Depth profiles of investigated conversion layers

The results from the XPS studies of the surface of the “as-deposited” formed conversion layers on Al substrate, subjected to different types of pretreatments are represented in Table 2. It follows from these results that these pretreatments of the substrates, and the composition of the solutions for the formation of mixed conversion layers, exert substantial impact on the concentrations of the two

components: Al_2O_3 and $\text{Ce}_2\text{O}_3+\text{CeO}_2$, building them up, as well as on the layer thickness (Fig. 4 and Fig. 5). This impact is notable with respect to the change in the ratio between Ce^{3+} (Ce_2O_3) and Ce^{4+} (CeO_2) in the conversion layers (Table 2). It is observed from the Table 2 that after pretreatment of the Al substrate only in NaOH, the concentration of Ce^{4+} is 26%, amounting to ~ 89% of the total concentration (29.1%) of Ce on the surface of the conversion layer. After consecutive treatment of the Al substrate in NaOH and HNO_3 the concentration of Ce^{4+} is 19%, which amounting to about 49% of the total concentration (39%) of Ce on the surface of the conversion film. Therefore, in the second case the quantity of strong corrosion-resistive CeO_2 [41] in the conversion layer is about two times higher than in the layer formed after pretreatment of the Al substrate in NaOH alone.

Analogous effect is also observed in the case when Cu^{2+} ions are present in the solution for deposition of conversion layers. After pretreatment of the Al substrate only in NaOH the concentration of Ce^{4+} on the surface of the conversion layer is 25%. This amounts to ~ 69% of the total concentration (36,2%) of Ce in it (Table 2). After consecutive treatments of the Al substrate in NaOH and in HNO_3 , the concentration of Ce^{4+} becomes 33,6%, which is ~ 96% of the total concentration of Ce (35%) on the surface of the conversion layer (Table 2).

Table 2. Chemical composition and ratio between the elements Al, O, Ce and Cu (in at.%) in the formed conversion layers depending on the type of pretreatment of the studied samples. All data are determined by XPS analysis (calculated from spectra obtained at 60 sec etching time with Ar^+ beam, not given here).

Type of sample	O	Al	Ce	Cu	Ce^{4+}	Ratio $\frac{\text{Ce}^{4+}}{(\text{Ce}^{3+}+\text{Ce}^{4+})}$
$\text{CeOx}_{\text{CeCl}_3}/\text{Al}_{\text{NaOH}}$	58.5	12.4	29.1	-	26.0	0.89
$\text{CeOx}_{\text{CeCl}_3}/\text{Al}_{\text{NaOH}/\text{HNO}_3}$	54.0	7.0	39.0	-	19.0	0.49
$\text{CeOx}_{\text{CeCl}_3+\text{CuCl}_2}/\text{Al}_{\text{NaOH}}$	60.4	0.0	36.2	3.4	25.0	0.69
$\text{CeOx}_{\text{CeCl}_3+\text{CuCl}_2}/\text{Al}_{\text{NaOH}/\text{HNO}_3}$	62.0	0.0	35.0	3.0	33.6	0.96

Clearly, the presence of Cu^{2+} ions in the solution for conversion treatment also leads to the deposition of some elementary copper on the Al substrate (Fig.3). The formed additional copper cathodic sections, as well as the catalytic action of the copper ions [26] in the solution (see also Fig.6) substantially facilitate the precipitation (equations 5 - 7) of the cerium oxide component of the conversion layer into $\text{Ce}(\text{OH})_4$, respectively - CeO_2 state. This reflects favorably upon the thickness and upon the content of the hardly soluble CeO_2 [42] in the mixed conversion layers (Fig.4 and Fig.5).

Figure 4 represents the results from the in-depth profiles made with the preliminarily treated in NaOH $\text{CeOx}_{\text{CeCl}_3}/\text{Al}_{\text{NaOH}}$ sample (Fig. 4a) and consecutively treated in HNO_3 $\text{CeOx}_{\text{CeCl}_3}/\text{Al}_{\text{NaOH}/\text{HNO}_3}$ sample (Fig. 4b), upon which a conversion coating has been deposited from solution, containing Ce^{3+} ions. These results indicate that the type of Al substrate surface pretreatment can influence substantially the kinetics of formation of the conversion CeO_x layers. The results from analogous investigations in the case when the conversion coating has been deposited from electrolyte containing

both Ce^{3+} and Cu^{2+} ions – samples $CeOx_{CeCl3+CuCl2}/Al_{NaOH}$ and $CeOx_{CeCl3+CuCl2}/Al_{NaOH/HNO3}$ - are illustrated in Figure 5a and 5b. One can see in the obtained in-depth profiles for these samples that the surface concentration of the conversion deposited ceria ($Ce_2O_3+ CeO_2$) layers also depends on this factor. The XPS analysis (Table 2) gives values of 26% and 19%, respectively for CeIVoxide (CeO_2) in the absence of copper ions and 25% and 34%, respectively - in the presence of copper ions in the conversion solution.

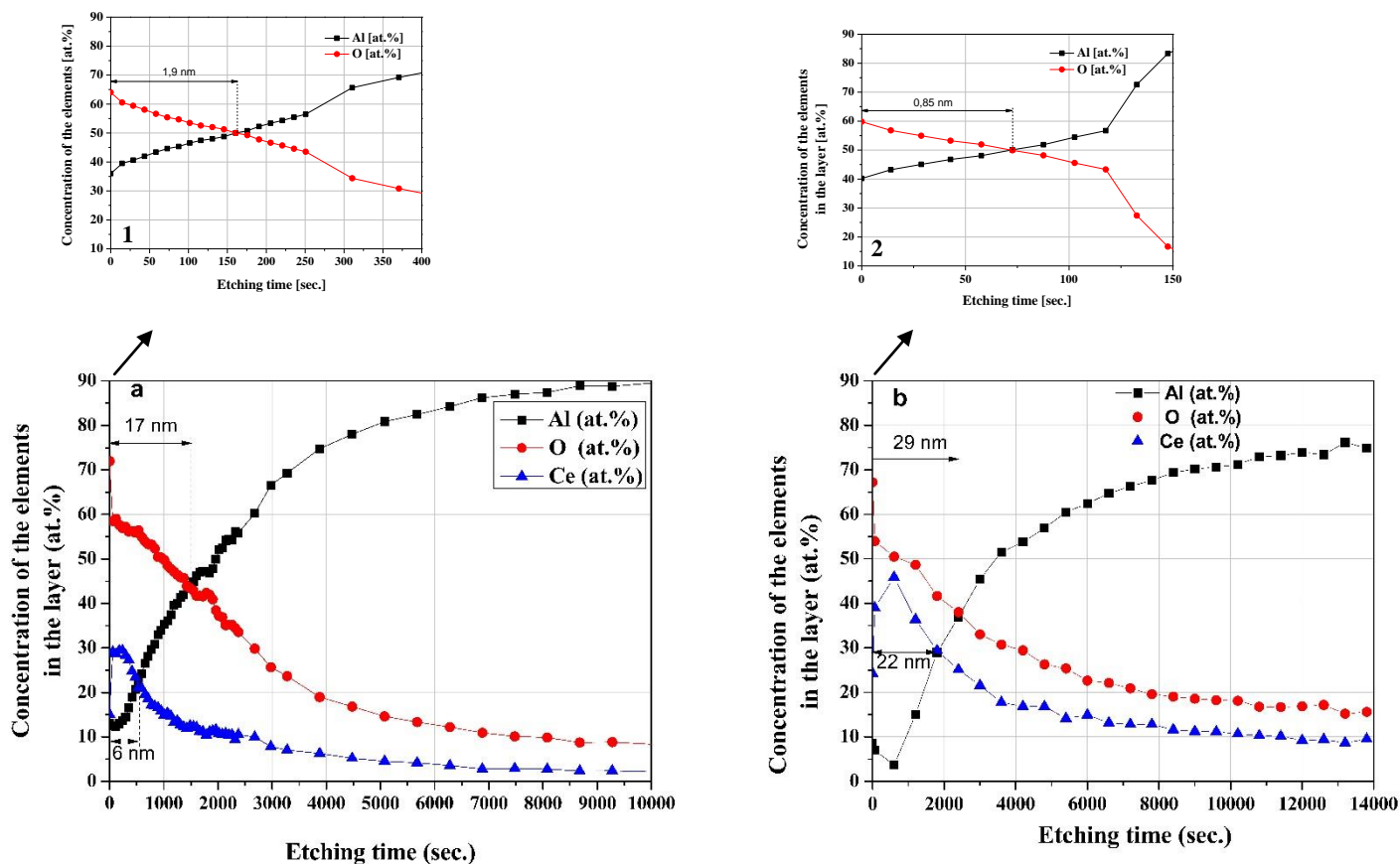


Figure 4. Depth profiles, displaying the change in the ratio between the elements Ce, Al and in the conversion layers (deposited from solution, containing only Ce^{3+} ions) on: (a) $CeOx_{CeCl3}/Al_{NaOH}$ sample and (b) $CeOx_{CeCl3}/Al_{NaOH/HNO3}$ sample. Depth profiles (inserts 1 and 2) show the change in the ratio between the elements Al and O in the surface layers formed on the Al substrate, after its pre-treatment in: 1 - 1.5M NaOH and 2 - 1.5M NaOH and 5M HNO_3 .

The juxtaposition of the in-depth profiles in regard to the thickness of the secondarily formed oxihydroxide/oxide layer on the aluminium substrate, after the pretreatment in NaOH [36], with the in-depth profile of the sample having deposited on it conversion cerium oxide layer from electrolyte containing only Ce^{3+} ions (Fig. 4a), shows that it consists of two components – ($Ce_2O_3- CeO_2$) and Al_2O_3 . The dominating one on the surface of the conversion layer is ($Ce_2O_3- CeO_2$) - until ~540 sec time interval of Ar^+ ions bombardment (equal to thickness of the conversion layer ~ 6 nm), while in the depth up to ~1500 sec time interval of Ar^+ bombardment (from 6th – 17th nm in depth), in close vicinity to the „Conversion layer ($Ce_2O_3-CeO_2$) + Al_2O_3/Al substrate“inter-phase boundary of the

system Al_2O_3 dominates (Fig. 4a). When Cu^{2+} ions have also been added in the solution for conversion treatment, this dependence is preserved. Thereupon the thickness of the cerium oxide film (which is dominating on the surface) is increased considerably - up to ~ 7500 sec time interval of Ar^+ bombardment (87 nm). Subsequently, in the depth up to about 9300 sec. time interval of Ar^+ bombardment (from 87 to 110 nm) $-\text{Al}_2\text{O}_3$ prevails (Fig.5 a).

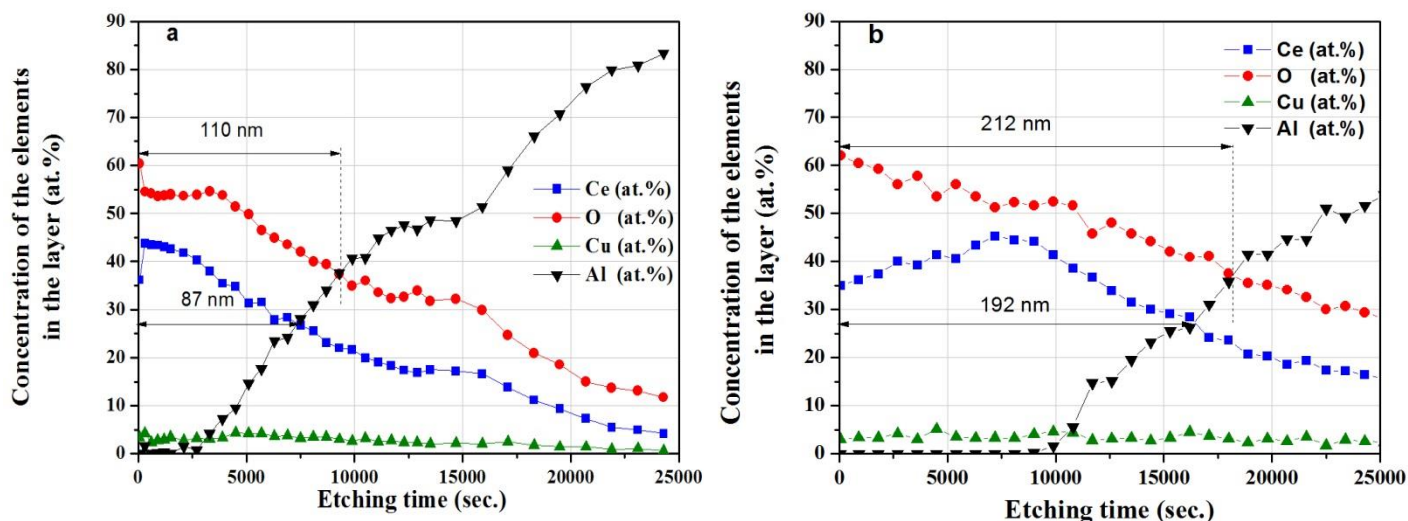


Figure 5. Depth profiles, showing the change in the ratio between the elements Ce, Cu, Al and O in the conversion layers (deposited from solution, containing Ce^{3+} and Cu^{2+} ions) on: (a) Al substrate, treated in solution of 1.5M NaOH - sample $\text{CeO}_x\text{CeCl}_3+\text{CuCl}_2/\text{Al}_{\text{NaOH}}$ and (b) Al substrate, treated consecutively in solution 1.5M NaOH and 5M HNO_3 - sample $\text{CeO}_x\text{CeCl}_3+\text{CuCl}_2/\text{Al}_{\text{NaOH/HNO}_3}$.

When the pretreatment consists of consecutive treatment steps in NaOH and in HNO_3 , the thickness of the oxihydroxide/oxide film formed during these two treatment steps upon the aluminium substrate, is twice smaller ($\sim 0.85\text{nm}$) [36]. Thereafter follows the formation of conversion cerium oxide film in electrolyte, containing only Ce^{3+} ions, and it also consists of two components - (Ce_2O_3 - CeO_2) and Al_2O_3 . In this case the domination of cerium oxide on the surface layer is significantly thicker in comparison with the case of pretreatment only with NaOH, reaching value up to ~ 1800 sec time interval of Ar^+ bombardment (equal to ~ 22 nm) - Fig.4 b. The next dominating in depth component (until ~ 2450 sec time interval of Ar^+ bombardment (corresponding to thicknesses from 22 to 29 nm)) is Al_2O_3 . When one also adds Cu^{2+} ions to the solution for conversion treatment, the dominating ceria layer on the surface becomes considerably thicker (detected up to ~ 16400 sec time interval of Ar^+ bombardment (equal to ~ 192 nm)) and thereafter in depth up to ~ 18300 sec time interval of Ar^+ bombardment (equal to ~ 212 nm) the mixed conversion film is dominated by Al_2O_3 component of the mixed conversion layer (Fig. 5b).

As mentioned above, the mixed film formed during the pretreatment steps in NaOH and in HNO_3 on the surface of the aluminum substrate, consists of $\text{AlOOH}/\text{Al}_2\text{O}_3$ (at an approximate ratio of 3.6 : 1) and it is much thinner than the conversion coating formed upon it, which represents a mixture

of Al_2O_3 and $(\text{Ce}_2\text{O}_3\text{-CeO}_2)$. The registered difference in the thicknesses of the conversion films after the two types of pretreatment of the Al substrate (in NaOH and consecutively in NaOH and in HNO_3) most probably could be associated with the appearance of larger number of active cathodic sections (intermetalides Al_3Fe) after the additional treatment with HNO_3 . On the basis of the obtained results about the changes in the composition of the conversion films in depth (Fig. 4. and Fig. 5), it follows that in the case of forming conversion coatings in electrolyte containing only Ce^{3+} ions, reactions (1 – 7) are proceeding, whereupon at the beginning reaction (4) is dominating, determining the formation of $\text{Al}(\text{OH})_3/\text{Al}_2\text{O}_3$ (Fig.6). However, subsequently reactions (5-7) become prevailing, which determines the formation of $\text{Ce}(\text{OH})_3/\text{Ce}(\text{OH})_4$ ($\text{Ce}_2\text{O}_3+\text{CeO}_2$) – Fig.6. Upon also adding copper ions in the cases of the samples, pretreated only in NaOH, the appearance of the $(\text{Ce}_2\text{O}_3\text{-CeO}_2)$ component of the mixed conversion layer (characterized by thickness of ~ 7500 sec time interval of Ar bombardment - equal to ~ 87 nm), there is total domination of the cerium oxide in the $(\text{Ce}_2\text{O}_3\text{-CeO}_2) + \text{Al}_2\text{O}_3$ conversion layer and its protective ability, respectively. The contribution of Al_2O_3 in this system is manifest at small thickness (during the period of initial growth) of the conversion layer until ~ 2000 sec time interval of Ar^+ bombardment (equal to ~ 23 nm) close to the interface of the „conversion layer $(\text{Ce}_2\text{O}_3\text{-CeO}_2) + \text{Al}_2\text{O}_3/\text{Al}$ substrate“ system (time interval of argon etching $\sim 7500 - 9300$ sec (thickness from 87 to 110 nm)). This change in the ratio $\text{Al}_2\text{O}_3: (\text{Ce}_2\text{O}_3\text{-CeO}_2)$ in the conversion layer, in our opinion, is also connected with the formation of much larger number of cathodic sections of copper (Fig. 6). As mentioned above (EDS data under Fig. 3), the formation of active cathodic sections of elementary copper on the Al substrate favorably influences the processes of formation of cerium oxide layer on the aluminium surface. Additionally, their presence accelerates the process of dissolution of Al – the anodic reaction (equation 3) of the immersion process [31,39]. This effect induces changes in the rate of the cathodic reaction of O_2 reduction (conjugated reaction of the immersion process – equations 1 and 2), which is in accordance with the electrochemical mechanism (Fig.6), assumed by us, and leads to increase in the quantity of deposited cerium hydroxide-oxide layers (equations 6 and 7) on the aluminium substrate.

The total number of cathodic sections in this case is much greater than the number of cathodic sections of Al_3Fe , operating in the conversion solution, containing no copper ions.

The above discussed dependence of the increase in the thickness of the conversion layers is manifest to even greater extent, when the pretreatment involves also treatment of the substrate in HNO_3 . In this case, the aluminum oxide component in the consecutive/mixed $(\text{Ce}_2\text{O}_3\text{-CeO}_2) + \text{Al}_2\text{O}_3$ conversion layer is observable in the time interval of layer-by-layer removal of the conversion film - ~ 18300 sec time interval of Ar^+ bombardment (equal to $\sim 212\text{nm}$) until ~ 10000 sec (equal to $\sim 117\text{nm}$) - over the surface of the „conversion layer $(\text{Ce}_2\text{O}_3\text{-CeO}_2) + \text{Al}_2\text{O}_3$ “/”Al substrate“ interface. In the film, removed layer-by-layer from the surface of the sample in depth (starting with 1 sec and reaching up to ~ 10000 sec. time interval of Ar bombardment (equal to ~ 117 nm)) in the conversion layer only the component $(\text{Ce}_2\text{O}_3\text{-CeO}_2)$ is being detected (Fig. 5b).

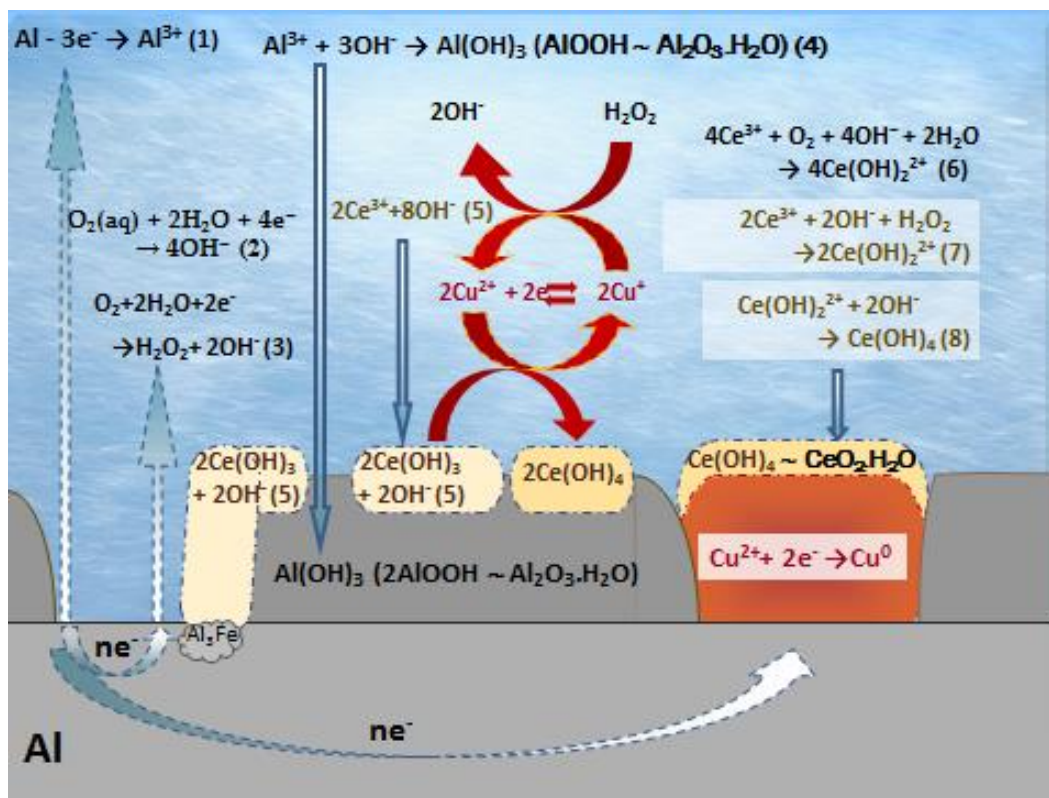


Figure 6. Scheme of the processes, occurring during deposition of cerium oxide(s) conversion layers on Al substrate from electrolytes, containing Ce³⁺ and Cu²⁺ ions.

3.3. Electrochemical investigations

3.3.1. Potentiodynamic polarization curves

It is seen that the conversion layers, formed on samples, activated preliminarily in NaOH, inhibit to a greater extent the cathodic depolarization reaction of the corrosion process (Fig.7 a, curve 2) in 0.1M NaCl compared to the films formed on samples subjected first to activation in solution of NaOH and subsequently to deoxidizing in HNO₃ (Fig. 7a, curve 3). This change in the course of the cathodic polarization curves indicates decrease in the rate of the reaction of reduction of oxygen, which is associated with substantial lowering of the corrosion currents (Table 3). Therefore, no passivity behaviour is observed in the anodic branch of the polarization curves. The calculated degree of corrosion protection *z*, on the basis of the values of the corrosion currents, determined in the model potentiodynamic investigations reaches a value of 93.75% (Table 3). This is proof that the formed mixed (Ce₂O₃-CeO₂) + Al₂O₃ conversion layer is a more efficient barrier to the corrosion process, in the case when the samples have been pretreated only in NaOH (Tables 2 and 3).

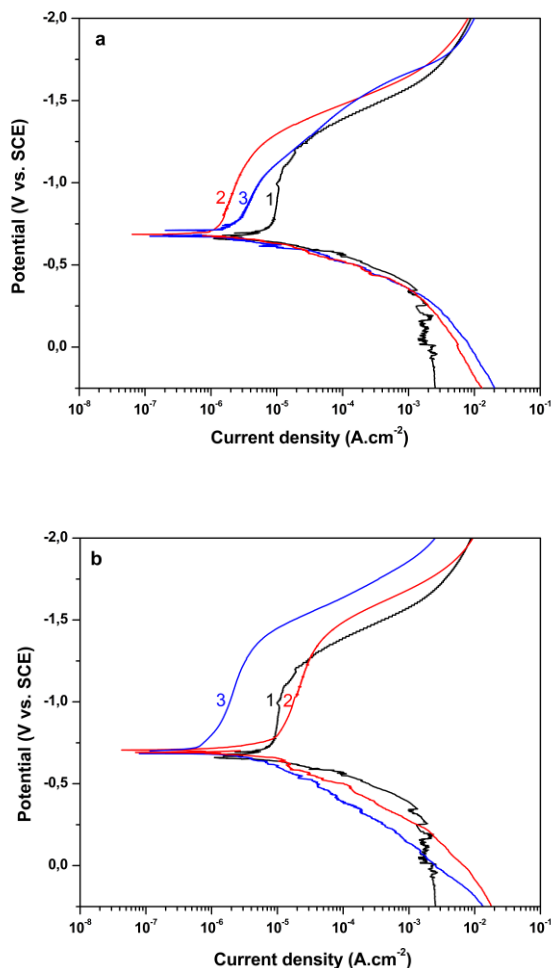


Figure 7. Polarization curves of the tested systems in 0.1M NaCl at 25 °C for the: a) samples $\text{Al}_2\text{O}_3\text{native}/\text{Al}$ (curve 1); $\text{CeOx}_{\text{CeCl}_3}/\text{Al}_{\text{NaOH}}$ (curve 2) and $\text{CeOx}_{\text{CeCl}_3}/\text{Al}_{\text{NaOH}/\text{HNO}_3}$ (curve 3) ;b) samples $\text{Al}_2\text{O}_3\text{native}/\text{Al}$ (curve 1); $\text{CeOx}_{\text{CeCl}_3+\text{CuCl}_2}/\text{Al}_{\text{NaOH}}$ (curve 2) and $\text{CeOx}_{\text{CeCl}_3+\text{CuCl}_2}/\text{Al}_{\text{NaOH}/\text{HNO}_3}$ (curve 3).

Table 3. Influence of the type of pretreatment operations of the Al substrate and chemical content of the solutions for deposition of conversion layers on the electrochemical parameters (determined from the potentiodynamic polarization curves) of the studied systems.

Type of sample	Corrosion potential, E_{corr} , V vs. SCE	Corrosion current, j_{corr} , Acm^{-2}	b_c , mVdec^{-1}	Degree of corrosion protection, z (%)
Al_2O_3 native/Al	-0.660	8×10^{-6}	65	-
$\text{CeOx}_{\text{CeCl}_3}/\text{Al}_{\text{NaOH}}$	-0.683	5×10^{-7}	190	93.75
$\text{CeOx}_{\text{CeCl}_3}/\text{Al}_{\text{NaOH}/\text{HNO}_3}$	-0.679	9×10^{-7}	178	88.75
$\text{CeOx}_{\text{CeCl}_3+\text{CuCl}_2}/\text{Al}_{\text{NaOH}}$	-0.701	1×10^{-6}	81	87.50
$\text{CeOx}_{\text{CeCl}_3+\text{CuCl}_2}/\text{Al}_{\text{NaOH}/\text{HNO}_3}$	-0.685	4×10^{-7}	396	95.00

The analogous polarization curves, obtained with samples, coated with conversion film from electrolyte containing CeCl_3 and CuCl_2 are represented in Figure 7b. In this case, when the samples have been treated in advance only in NaOH , the conversion treatment leads to insignificant decrease in the corrosion current. The protective ability of the conversion film is substantially improved, when the samples were treated consecutively in NaOH first and then in HNO_3 . The additional acidic deoxidizing results in the formation of conversion films acting as efficient cathodic inhibitors (Fig. 7b, curve 3). In such a case, the degree of corrosion protection against corrosion reaches the value of 95%, which is evidence for the importance of the acidic preliminary treatment of the Al substrate as a favourable factor during the formation of $(\text{Ce}_2\text{O}_3\text{-CeO}_2) + \text{Al}_2\text{O}_3$ conversion films on their surface.

3.3.2. Chronoamperometric investigations

Fig. 8 presents the results of the chronoamperometric investigations using the obtained samples, polarized anodically at potential of -0.5 V (vs. SCE) – the potential of pitting formation on the studied aluminum in 0.1 M NaCl [42]. In these experiments, polarizing the samples anodically in a medium, containing chloride anions, we aimed to approach to a maximal extent the actual corrosion process respectively corrosion characterization in view of pitting corrosion, which is characteristic of aluminum and its alloys. Based on the course of the registered curves we could judge the character of the corrosion attack and the appearance of pitting damages.

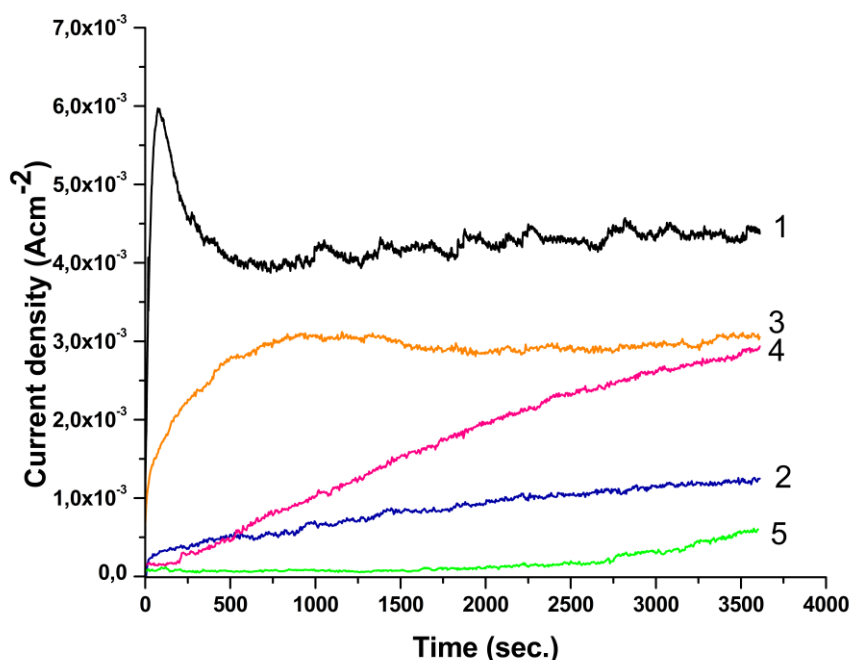


Figure 8. Chronoamperometric curves of the studied samples: 1 – $\text{Al}/\text{Al}_2\text{O}_3$ native; 2 – $\text{CeOx}_{\text{CeCl}_3}/\text{Al}_{\text{NaOH}}$; 3 – $\text{CeOx}_{\text{CeCl}_3}/\text{Al}_{\text{NaOH}/\text{HNO}_3}$; 4 – $\text{CeOx}_{\text{CeCl}_3+\text{CuCl}_2}/\text{Al}_{\text{NaOH}}$; 5 – $\text{CeOx}_{\text{CeCl}_3+\text{CuCl}_2}/\text{Al}_{\text{NaOH}/\text{HNO}_3}$ in 0,1M NaCl at the pitting potential of Al (-0.5 V vs. SCE).

We observed that for the aluminum samples without pretreatment (sample $\text{Al}_2\text{O}_{3\text{native}}/\text{Al}$), after its immersion at the potential of pitting formation [42] in the corrosive medium, the corrosion current density is sharply increased (until reaching the ~ 100 -th second of exposure to corrosive medium) up to values $\sim 6 \cdot 10^{-3} \text{ A}\cdot\text{cm}^{-2}$, whereupon the natural passive film is disrupted on the aluminum surface (Fig. 8, curve 1), which is a prerequisite for the appearance and development of pitting corrosion during the interaction with the corrosive medium. After breaking through the passive film, there starts a process of local corrosion characterized by values of the anodic current (j_a) $\sim 4,35 \cdot 10^{-3} \text{ A}\cdot\text{cm}^{-2}$ and current oscillations specific for it, owing to unstable pittings which are repassivated/activated.

The behavior of the samples subjected to pretreatment, upon which a protective conversion layer is formed, is illustrated by the curves 2 – 5 in Fig.8. The curves 2 and 3 characterize the anodic (corrosion) behaviour of the samples $\text{CeOx}_{\text{CeCl}_3}/\text{Al}_{\text{NaOH}}$ and $\text{CeOx}_{\text{CeCl}_3}/\text{Al}_{\text{NaOH}/\text{HNO}_3}$, which have respectively been treated in advance in NaOH or first in NaOH and in then HNO_3 , with conversion layers formed in solutions, containing only Ce^{3+} ions. Curves 4 and 5 (samples $\text{CeOx}_{\text{CeCl}_3+\text{CuCl}_2}/\text{Al}_{\text{NaOH}}$; and $\text{CeOx}_{\text{CeCl}_3+\text{CuCl}_2}/\text{Al}_{\text{NaOH}/\text{HNO}_3}$) in Fig. 8 characterize the anodic behavior of the samples that have been treated in advance by the same sequence, and thereafter a conversion layer is formed in solution containing Ce^{3+} and Cu^{2+} ions. Judging from the course of curve 2, one could conclude that after the pretreatment of the Al substrate only in NaOH, conversion protective layer deposited from solution containing only Ce^{3+} determines the several times higher protective effect with respect to pitting corrosion - $j_a \sim 1,16 \cdot 10^{-3} \text{ A}\cdot\text{cm}^{-2}$ (on the 3000th second of exposure to the corrosive medium). This substantial decrease in the corrosion current at the preset potential of pitting formation, its gradual alteration/enhancement with the course of time, as well as the diminishing amplitude of the fluctuations of the corrosion current can be associated with the protective action of the conversion layer. In depth it is characterized by the domination of the cerium oxide film in the protection of the Al substrate. This is valid until the time interval of etching by a beam of argon ions becomes ~ 1500 s, respectively thickness of the conversion layer ~ 5 -6 nm. Thereafter - starting from the 540th sec until ~ 1500 sec of etching by a beam of argon ions, its aluminum oxide component becomes dominating - respectively the thicknesses of the conversion layer is ~ 17 nm – Fig. 4a and Table 1. While after the consecutive pretreatment of the Al substrate in NaOH and HNO_3 (curve 3), the protective effect of the conversion layer deposited from solution containing only Ce^{3+} is weaker and it is stabilized only after about the 750th sec of exposure to the corrosive medium. Thereupon, the values of j_a are $\sim 2,93 \cdot 10^{-3} \text{ A}\cdot\text{cm}^{-2}$. In accordance with the depth profiles (Fig. 4b), the thickness of the conversion layer, however, is with about 60% greater in comparison with the layer, represented in Fig. 4 a (1500s vs. 2500 s of etching using a beam of argon ions). At the same time, the change in the concentration, respectively in the ratio between the cerium oxides and the aluminum oxide components in the conversion layer (Fig. 4 b, Table 2), shows a double decrease in the content of the aluminum oxide component in the conversion layer in comparison with the rate, when the pretreatment of the Al substrate has been accomplished only in a solution of NaOH (Fig. 4.a).

When after the pretreatment of the Al substrate only in solution of NaOH the formation of the conversion layer is accomplished in a working electrolyte containing both Ce^{3+} and Cu^{2+} ions, the deposited conversion layers (after exposure under the conditions of anodic polarization at the potential of pitting formation) are characterized by $j_a \sim 2,63 \cdot 10^{-3} \text{ A}\cdot\text{cm}^{-2}$ (Fig. 8, curve 4). At the same time no

current fluctuations characteristic for pitting formation are observed. The best corrosion behavior under the conditions of anodic polarization was observed with the conversion films obtained after consecutive pretreatments first in NaOH and HNO₃ – sample CeOx_{CeCl3+CuCl2}/Al_{NaOH/HNO3} (Fig. 8, curve 5). In this case, the anodic currents preserve very low values ($j_a \sim 2,92 \cdot 10^{-4}$ A.cm⁻² - on the 3000th second of exposure to the corrosive medium). There within the entire time interval of the investigation no oscillations characterizing pitting break through the conversion protective layer have been observed. It is important to note that with both formed conversion protective layers upon etching with argon ions beam no presence of an aluminum oxide component of the conversion layer was registered until etching time intervals respectively ~ 2450 s and 10 000 s, which correspond to thicknesses of 29 nm and 117 nm, respectively. In these cases the cerium oxide component is dominant in the protective ability of the conversion layer of thicknesses up to 7500 sec ($\delta \sim 87$ nm), while the aluminium oxide component is found in close vicinity ($\delta \sim 20$ nm) to the interface of the „conversion layer (Ce₂O₃-CeO₂)+Al₂O₃/Al substrate“ system. The additional treatment in HNO₃ promotes these values until 16400 sec. time interval of Ar bombardment (equal to ~192 nm) and 18300 sec time interval of Ar bombardment (equal to ~ 212 nm), respectively.

The juxtaposition of the chronoamperograms shows that the order of stabilities of the systems towards the appearance and development of pitting corrosion is the following: Al₂O_{3native}/Al < CeOx_{CeCl3}/Al_{NaOH/HNO3} < CeOx_{CeCl3+CuCl2}/Al_{NaOH} < CeOx_{CeCl3}/Al_{NaOH} < CeOx_{CeCl3+CuCl2}/Al_{NaOH/HNO3}.

5. CONCLUSIONS

Comparing the above given order of increasing corrosion protection abilities of the studied conversion layers with the data on: corrosion parameters and the degree of corrosion protection; XPS results and profiles in depth; and the chronoamperometric measurements - the following conclusions can be made:

- The conversion films, characterized by the highest protection ability, were deposited after consecutive pretreatment of the substrate in NaOH and in HNO₃ and formation of the conversion layer in solution, containing both Ce³⁺ and Cu²⁺ ions. Their specific feature is that they are a mix between Al₂O₃ and Ce₂O₃+CeO₂. The thickness of these conversion layers is the greatest and the cerium oxide component is dominating in their composition.

- Lower protection ability was registered, when the pretreatment of the substrate was accomplished only in solution of NaOH and the formation of the conversion layer was carried out in solution, containing only Ce³⁺ ions. Characteristic feature in this case is that the thickness of the conversion layer is considerably smaller, and the dominating component in it is the aluminium oxide.

- When the pretreatment of the Al substrate was realized only in solution of NaOH and the formation of the conversion layer was done in solution containing simultaneously Ce³⁺ and Cu²⁺ ions, a much faster decrease in the protection ability was observed in the course of time of exposure to the corrosive medium. In this case, although the thickness of the conversion layer is about five times greater, the protection ability is decreasing relatively faster. The reason for this is the incomplete

„screening“ with cerium oxide layer of the deposited on Al substrate copper clusters, respectively the negative functioning of the galvanic Cu/Al couples.

- The data from the X-ray photoelectron spectroscopy study and depth profiles of investigated conversion layers show in a unique way, that the determining factor for the protection ability of the studied mixed conversion layer is the content of Ce^{4+} , i.e. the respectively CeO_2 component, in them.

ACKNOWLEDGEMENT

The authors acknowledge thankfully the financial support by the project Program for career development of young scientists, BAS 2016 and by NSF BG Contract T 02/22.

References

1. P.S. S. Wernick, R. Pinner, 5th ed., ASM International and Finishing Publications Ltd. Metals Park, Ohio, 1987.
2. L. Patrick, Hagans, Naval, Research, Laboratory, Christina, M., Haas, *Chromate Conversion Coatings, Surf. Eng.* 5 (1994) 405.
3. R. Berger, U. Bexell, T. Mikael Grehk, S.E. Hörnström, *Surf. Coatings Technol.* 202 (2007) 391.
4. N.-T. Wen, C.-S. Lin, C.-Y. Bai, M.-D. Ger, *Surf. Coatings Technol.* 203 (2008) 317
5. J. Da Fonte, C. Mich, US Patent 4 359 345, 1982.
6. G.D. Wilcox, D.R. Gabe, M.E. Warwick, *Corros. Sci.* 28 (1988) 577
7. P.D. Deck, D.W. Reichgott, B. Metchem, T. Pa, *Met. Finish.* 90 (1992) 29.
8. B.R.W. Hinton, *Met. Finish.* 89 (1991) 15.
9. M. Delucchi, A. Barbucci, T. Temtchenko, T. Poggio, G. Cerisola, *Prog. Org. Coatings.* 44 (2002) 261.
10. A. Barbucci, M. Delucchi, G. Cerisola, *Prog. Org. Coatings.* 33 (1998) 131.
11. M.F. Montemor, A.M. Simões, M.J. Carmezim, *Applied Surface Science* 253 (2007) 6922.
12. M.F. Montemor, A.M. Simões, M.G.S. Ferreira, M.J. Carmezim, *Applied Surface Science* 254 (2008) 1806.
13. M. Balasubramanian, C.A. Melendres, A.N. Mansour, *Thin Solid Films.* 347 (1999) 178.
14. N.E. Hinton, B.R.W., Arnott, D.R., Ryan, *Mater. Forum.* 9 (1986) 162.
15. L. Wilson, B.R.W. Hinton, Patent WO, 88 066 399 (1988).
16. A.E. Hughes, R.J. Taylor, B.R.W. Hinton, L. Wilson, *Surf. Interface Anal.* 23 (1995) 540.
17. C.M. Rangel, T.I. Paiva, P.P. da Luz, *Surf. Coatings Technol.* 202 (2008) 3396.
18. C.E. Castano, M.J. O'Keefe, W.G. Fahrenholtz, *Curr. Opin. Solid State Mater. Sci.* 19 (2015) 69.
19. M. Machkova, E.A. Matter, S. Kozhukharov, V. Kozhukharov, *Corros. Sci.* 69 (2013) 396.
20. E.A. Matter, S. Kozhukharov, M. MacHkova, V. Kozhukharov, *Mater. Corros.* 64 (2013) 408.
21. T.G. Harvey, *Corros. Eng. Sci. Technol.* 48 (2013) 248.
22. A.J. Aldykewicz, H.S. Isaacs, A.J. Davenport, *J. Electrochem. Soc.* 142 (1995) 3342.
23. X.-W. Yu, C.-N. Cao, *Trans. Nonferrous Met. Soc. China* (English Ed. 10 (2000) 580.
24. X. Yu, C. Cao, Z. Yao, D. Zhou, Z. Yin, *Mater. Sci. Eng. A.* 284 (2000) 56.
25. X. Yu, C. Cao, Z. Yao, D. Zhou, Z. Yin, *Corros. Sci.* 43 (2001) 1283.
26. A. Decroly, J.P. Petitjean, *Surf. Coatings Technol.* 194 (2005) 1.
27. A.J. Aldykewicz, A.J. Davenport, H.S. Isaacs, *J. Electrochem. Soc.* 143 (1996) 147.
28. P. Campestrini, H. Terryn, A. Hovestad, J.H.W. de Wit, *Surf. Coatings Technol.* 176 (2004) 365.
29. F.H. Scholes, C. Soste, A.E. Hughes, S.G. Hardin, P.R. Curtis, *Appl. Surf. Sci.* 253 (2006) 1770
30. S. Joshi, W.G. Fahrenholtz, M.J. O'Keefe, *Appl. Surf. Sci.* 257 (2011) 1859

31. R. Andreeva, E. Stoyanova, A. Tsanev, P. Stefanov, D. Stoychev, *Trans. IMF*. 92 (2014) 203.
32. L.E.M. Palomino, J.F.W. De Castro, I. V. Aoki, H.G. De Melo, *J. Braz. Chem. Soc.* 14 (2003) 651.
33. A.E. Hughes, K.J.H. Nelson, *Inst. Met. Finish.* (1996) 241.
34. J. Trolho, T. Schmidt-Hansberg, P. Schubach, J. Trolho, *Alum. Extrus.* 8 (2003) 46.
35. A.S. Hamdy, A.M. Beccaria, P. Traverso, *Surf. Interface Anal.* 34 (2002) 171.
36. R. Andreeva, E. Stoyanova, A. Tsanev, D. Stoychev, *Journal of Physics: Conference Series* 700 (2016) 012049.
37. R. Andreeva, E. Stoyanova, D. Stoychev, *J. Int. Sci. Publ. Mater. Methods Technol.* 8 (2014) 751.
38. R. Lukanova, E. Stoyanova, M. Damyanov, D. Stoychev, *Bulg. Chem. Commun.* 40 (2008) 340.
39. E. Stoyanova, D. Stoychev, *J. Appl. Electrochem.* 27 (1997) 685.
40. F. Øvari, L. Tomcsányi, T. Túrmezey, *Electrochim. Acta.* 33 (1988) 323.
41. Jacob Ugay, *General and Inorganic Chemistry (In Russian)* Vyshaya shkola (1997) 527
42. Z. Szklarska-Smialowska, *Corros. Sci.* 41 (1999) 1743.

© 2018 The Authors. Published by ESG (www.electrochemsci.org). This article is an open access article distributed under the terms and conditions of the Creative Commons Attribution license (<http://creativecommons.org/licenses/by/4.0/>).